Chitosan Oligosaccharide-Stabilized Ferrimagnetic Iron Oxide Nanocubes for Magnetically Modulated Cancer Hyperthermia

Ki Hyun Bae,[†,#] Mihyun Park,[‡,#] Min Jae Do,[†] Nohyun Lee,[‡] Ji Hyun Ryu,[§] Gun Woo Kim,[⊥] CheolGi Kim,[⊥] Tae Gwan Park,[†,§] and Taeghwan Hyeon[‡,*]

[†]Department of Biological Sciences, Korea Advanced Institute of Science and Technology, Daejeon 305-701, Korea, [‡]School of Chemical and Biological Engineering and World Class University Program of Chemical Convergence for Energy & Environment, Seoul National University, Seoul 151-744, Korea, [§]Graduate School of Nanoscience and Technology, Korea Advanced Institute of Science and Technology, Daejeon 305-701, Korea, and [⊥]Department of Materials Science and Engineering, Chungnam National University, Daejeon 305-764, Korea. [#]These authors contributed equally to this work.

ABSTRACT

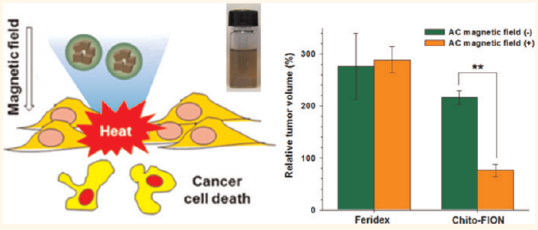

Magnetic nanoparticles have gained significant attention as a therapeutic agent for cancer treatment. Herein, we developed chitosan oligosaccharide-stabilized ferrimagnetic iron oxide nanocubes (Chito-FIONs) as an effective heat nanomediator for cancer hyperthermia. Dynamic light scattering and transmission electron microscopic analyses revealed that Chito-FIONs were composed of multiple 30-nm-sized FIONs encapsulated by a chitosan polymer shell. Multiple FIONs in an interior increased the total magnetic moments, which leads to localized accumulation under an applied magnetic field. Chito-FIONs also exhibited superior magnetic heating ability with a high specific loss power value (2614 W/g) compared with commercial superparamagnetic Feridex nanoparticles (83 W/g). The magnetically guided Chito-FIONs successfully eradicated target cancer cells through caspase-mediated apoptosis. Furthermore, Chito-FIONs showed excellent antitumor efficacy on an animal tumor model without any severe toxicity.

KEYWORDS: chitosan · magnetite · magnetic modulation · nanocube · cancer therapy · hyperthermia

Magnetic nanomaterials have attracted tremendous attention for their diverse biomedical applications including biological sensing, pathogen separation, intracellular drug delivery, and disease diagnosis.[1−6] Especially, uniform-sized and highly crystalline iron oxide nanoparticles are one of the most fascinating materials because of their tunable nanomagnetism and superior biocompatibility.[7−9] For example, various superparamagnetic iron oxide nanoparticles have been actively explored as efficient T_2 contrast agents for magnetic resonance imaging (MRI).[4,5] Furthermore, hollow-shaped iron oxide nanoparticles have gained significant attention as advanced drug delivery vehicles capable of carrying a large amount of anticancer medicines in the interior.[5,6]

Magnetic hyperthermia using ferrite nanoparticles has recently emerged as a promising therapeutic approach for cancer treatment. Ferrite nanoparticles can serve as tumor-destroying hyperthermia agents due to their ability to generate heat efficiently when exposed to an external alternating current (ac) magnetic field.[10−19] In contrast to the traditional hyperthermia therapies such as photothermal and radiofrequency ablation, magnetic hyperthermia provides a minimally invasive way to deliver a therapeutic dose of heat specifically to cancerous regions.[20,21] For clinically available hyperthermia, the development of efficient hyperthermia agents is of utmost importance. There have been many attempts to enhance the heating efficiencies of ferrite nanoparticles by controlling the magnetic domain size[18,19] and the magnetocrystalline anisotropy of the particles.[17,22] Recently, the Hyeon group reported the synthesis of uniform-sized ferrimagnetic iron oxide nanocubes (FIONs).[23] The magnetic properties of FIONs can be tuned from weak ferrimagnetic to strong ferrimagnetic by varying their sizes from 20 to 160 nm. Owing to their large magnetization and

* Address correspondence to thyeon@snu.ac.kr.

Received for review March 9, 2012 and accepted May 15, 2012.

Published online May 15, 2012
10.1021/nn301046w

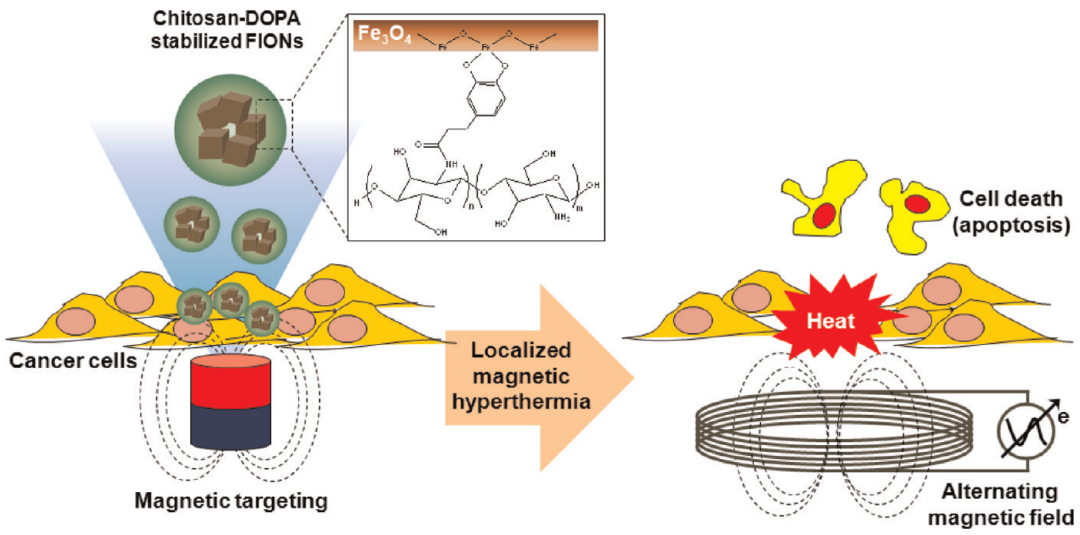

Figure 1. Schematic illustration of Chito-FIONs and their applications for the localized magnetic hyperthermia of cancer cells.

high relaxivity, 60-nm-sized FIONs have been successfully applied for MRI-based tracking of transplanted pancreatic islets at the single-cell level.[24] It has been reported that particles with a high size uniformity, large magnetization, and low coercivity are favorable for magnetic hyperthermia.[10,19] In this context, a 30-nm-sized FION is a particularly attractive candidate for effective thermotherapy because it has high colloidal stability in aqueous environments while maintaining a narrow particle-size distribution. Furthermore, the 30-nm-sized FIONs are expected to exhibit more effective heat dissipation than FIONs of larger size due to their higher saturation magnetization and lower coercivity.[23]

Chitosan is a natural polymer consisting of glucosamine and *N*-acetyl-D-glucosamine and has been widely exploited for biomedical and pharmaceutical applications due to its biocompatible, biodegradable, and bioactive properties.[25] In particular, chitosan oligosaccharide has been introduced to various types of nanoparticles to improve their colloidal stability and *in vivo* blood circulation.[26] With the aim of developing an effective nanotherapeutic agent highly stable in physiological environments, L-3,4-dihydroxyphenylalanine (DOPA)-conjugated chitosan oligosaccharide (chitosan-DOPA) is synthesized. DOPA is an unusual amino acid particularly abundant in adhesive proteins secreted by blue marine mussels (*Mytilus edulis*).[27] Since the catechol side chain of DOPA exhibits extremely strong affinity to diverse metal oxide surfaces through coordination bonding,[28−30] chitosan-DOPA is expected to be covalently anchored on the surface of FIONs *via* the mussel-inspired adhesion. Herein, we report on the applications of chitosan oligosaccharide-stabilized ferrimagnetic iron oxide nanocubes (Chito-FIONs) as a novel nanotherapeutic agent for hyperthermic cancer treatment.

RESULTS AND DISCUSSION

The Chito-FIONs are composed of a chitosan-DOPA polymeric shell encapsulating multiple FIONs in the interior (Figure 1). These novel nanomaterials are designed to be magnetically guided to the desired sites and activated remotely by an external ac magnetic field to generate localized cytotoxic heat. As a result, they can efficiently eradicate the target cancer cells *via* apoptosis-mediated tumoricidal effects.[21] This magnetically modulated hyperthermia has the potential to be applied as a promising approach for cancer treatment. Since the use of focused magnetic field gradients to attract Chito-FIONs toward tumors will allow the thermal energy to be restricted only in the tumor area, it is envisioned to destroy the tumors selectively while avoiding damage to healthy tissues. In the current study, we demonstrate that Chito-FIONs have superior magnetic heating ability and anticancer activities compared to the commercially available superparamagnetic iron oxide nanoparticles. Furthermore, their therapeutic potential was also evaluated on an animal tumor model in terms of tumor volume regression and prolonged residence in tumor sites.

Chitosan-DOPA was synthesized by conjugating a carboxylic acid group of hydrocaffeic acid to amino groups of chitosan oligosaccharide using carbodiimide chemistry. The degree of substitution determined by ^{1}H NMR spectroscopy was 31%, indicating that approximately eight DOPA moieties were conjugated to a single chitosan molecule (Figure S1, Supporting Information). Accordingly, it was conceivable that chitosan-DOPA molecules possessing multiple catechol binding units would be efficiently immobilized onto the surface of FIONs through multivalent bonding to the iron oxide nanostructures. For the preparation of Chito-FIONs, monodisperse oleic acid-capped FIONs with an average size of 30 nm were synthesized in

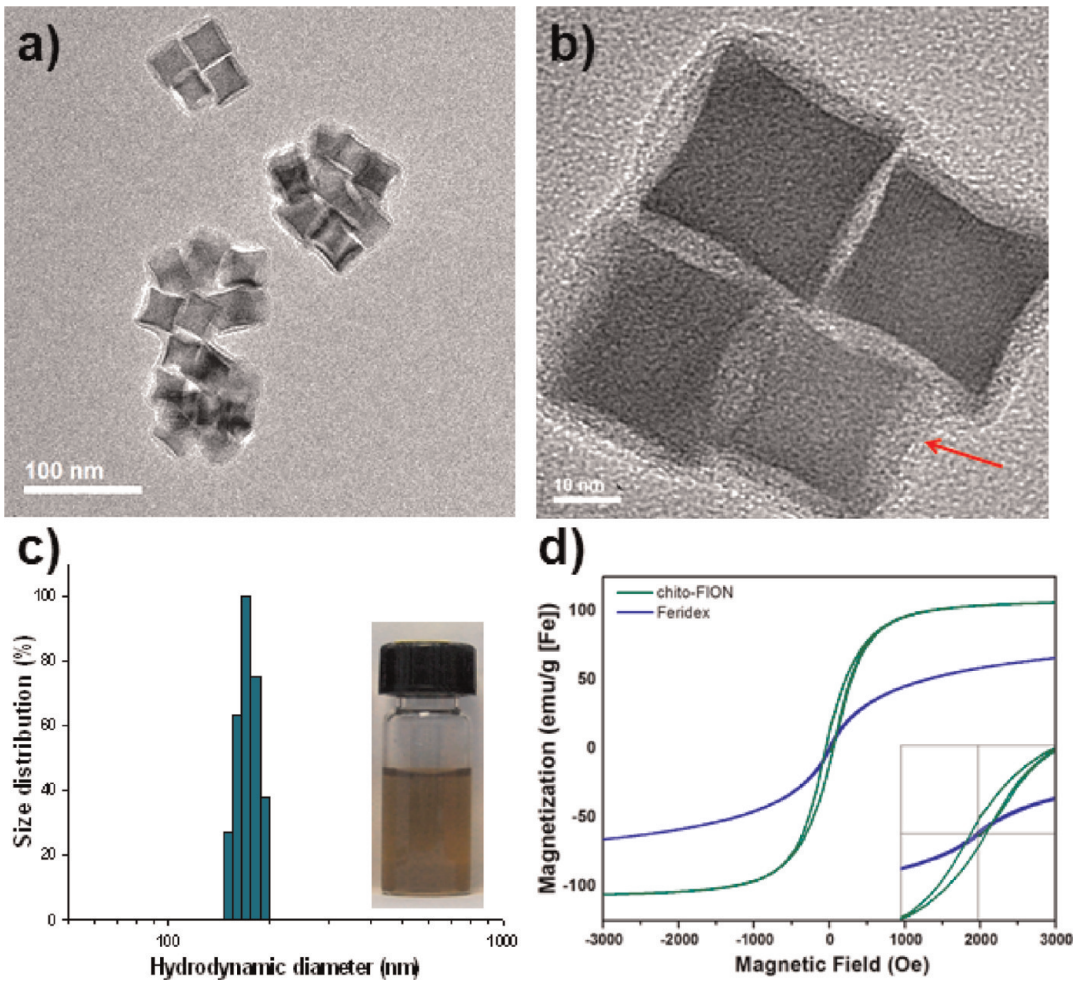

Figure 2. (a, b) TEM images of Chito-FIONs (red arrow indicates the presence of the polymer coating layers.) (c) Hydrodynamic diameters of Chito-FIONs in phosphate-buffered saline solution. Inset: Photograph showing the aqueous dispersion of Chito-FIONs. (d) Field-dependent magnetization curves of Chito-FIONs and Feridex.

organic solvent by the thermal decomposition process.[23] These oleic acid-capped FIONs dispersed in chloroform were added to an aqueous chitosan-DOPA solution and then subjected to ultrasonication to form an oil-in-water (O/W) emulsion, where the hydrophobic FIONs were localized inside oil-phase droplets. Upon evaporation of the residual solvent in the droplets, the multivalent binding of chitosan-DOPA to the iron oxide surfaces led to the immediate formation of water-dispersible Chito-FIONs stabilized with chitosan oligosaccharide.

The size and shape of Chito-FIONs were examined by transmission electron microscopy (TEM). Figure 2a shows the formation of well-dispersed Chito-FIONs encapsulated with multiple 30-nm-sized FIONs. The number of FIONs in a single Chito-FION particle was found to be 4−10. It was also observed that Chito-FIONs had a roughly spherical morphology with an average diameter of 103 ± 15 nm. The high-resolution TEM image (Figure 2b) revealed the presence of the uniform chitosan coating layers on the surface of FIONs, whereas no polymeric layer was observed around pristine FIONs (Figure S2, Supporting Information). To evaluate the hydrodynamic size of Chito-FIONs in an aqueous solution, dynamic light scattering (DLS) analysis was performed. The hydrodynamic diameter of Chito-FIONs (158 ± 17 nm) was slightly larger than the sizes observed in the TEM images, which was likely attributed to the expansion of hydrophilic chitosan shell layers in aqueous media (Figure 2c).[26] Moreover, it can be seen that the aqueous dispersion of Chito-FIONs yields a transparent brown solution without showing any aggregation, indicative of their excellent stability in an aqueous solution (Figure 2c, inset photograph). A FT-IR spectrum of Chito-FIONs showed strong absorption bands corresponding to the C−N stretch of chitosan and C═C vibration of catechol rings (Figure S3, Supporting Information). In addition, Chito-FIONs were shown to possess a positively charged surface with a ζ potential value of +50 ± 4 mV, confirming that cationic chitosan oligosaccharides were stably coated on the surface of FIONs. Multivalent catechol binding and/or electrostatic interactions between the positively charged

chitosan backbones and negatively charged iron oxide surface might play an important role in the successful immobilization of chitosan oligosaccharides on FIONs.[30] The magnetic properties of Chito-FIONs were investigated by measuring the magnetization as a function of the applied field at 300 K (Figure 2d). Chito-FIONs exhibited ferrimagnetic behavior, as indicated by the presence of open hysteresis loops in the M−H curves. Little change in the magnetic properties was observed between as-synthesized FIONs and Chito-FIONs, suggesting that the ferrimagnetic properties of FIONs were maintained after the ligand exchange with chitosan-DOPA (Figure S4, Supporting Information). It was also found that Chito-FIONs displayed higher saturation magnetization than that of commercially available Feridex. Such high saturation magnetization of Chito-FIONs is advantageous for magnetic guiding applications because it allows them to respond rapidly to an external magnetic field.[31]

To validate the applicability of Chito-FIONs for magnetic hyperthermia, their magnetic heating effect was evaluated under an ac magnetic field at a frequency of 1 MHz (Figure 3a). In the present study, a commercially available superparamagnetic iron oxide nanoparticle (Feridex) was chosen as a reference material for the magnetic hyperthermia studies.[32] When the Chito-FION solution (150 μg Fe/mL, 0.5 mL) was exposed to the ac magnetic field, the temperature increased rapidly and reached the therapeutic threshold required for cancer hyperthermia (T > 42 °C) within 10 min. In contrast, the temperature of the Feridex solution was not raised above 42 °C even after 20 min of exposure, which is insufficient to attain tumoricidal effects.[15] Although both Chito-FION and Feridex induced a temperature rise in a concentration-dependent manner, Chito-FION was more efficient in increasing the temperature than Feridex (Figure S5, Supporting Information). It is worth noting that Chito-FIONs had far greater hyperthermal efficiency than Feridex (Figure 3b). The specific loss power (SLP) value of Chito-FIONs (2614 W/g) was more than 30 times higher than that of Feridex (83 W/g). The influence of particle clustering on the hyperthermal efficiency was investigated by comparison with single-core FIONs coated by polyethylene glycol (PEG)-conjugated phospholipids.[24] The single-core FIONs were found to have a much lower SLP value (1792 W/g) than that of Chito-FIONs (Figure S6, Supporting Information). The improved heat generation ability of Chito-FIONs was likely related to the magnetic dipolar coupling between the neighboring FIONs in the interior of the Chito-FION particle.[33,34] As the dipole−dipole interactions become stronger with increasing particle density, the strengthened magnetic dipolar coupling of such particle ensembles could partially enhance the coercive field and stabilize the magnetization of the

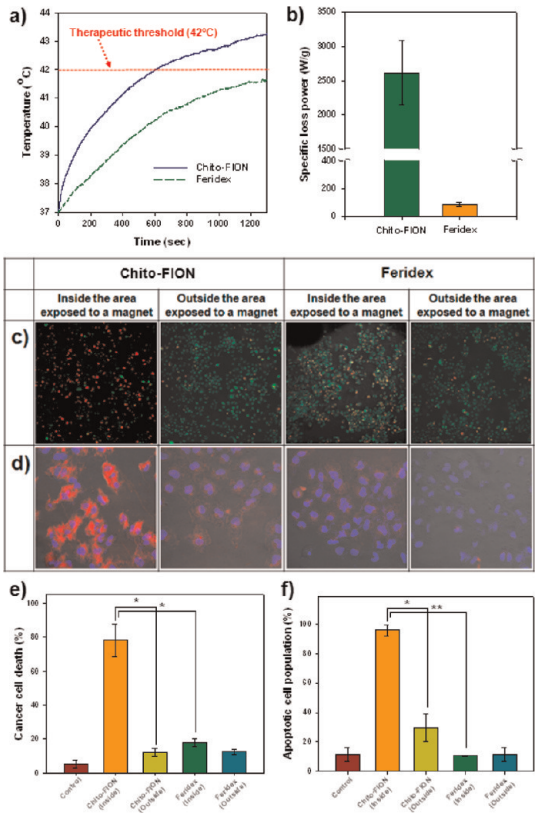

Figure 3. (a) Temperature *versus* time graphs of Chito-FIONs and Feridex dispersion (0.5 mL, 150 μg Fe/mL) under an ac magnetic field. (b) Specific loss power (SLP) values of Chito-FIONs and Feridex. (c) Confocal microscopic images of A549 cells following magnetic targeting with Chito-FIONs or Feridex and subsequent application of an ac magnetic field. The cells were stained with calcein AM (2 μM) and ethidium homodimer-1 (4 μM) for 30 min. Live and dead cells appear green and red, respectively. (d) Cellular apoptotic activity was detected by using a red fluorogenic substrate for caspases 3 and 7. Cell nuclei were also stained with DAPI (blue fluorescence). (e) Cell death and (f) apoptosis of A549 cells induced by the localized magnetic hyperthermia with Chito-FIONs or Feridex. Statistically significant difference between two groups, *p < 0.01, **p < 0.001.

individual FIONs, which in turn contributed to the remarkably high SLP value of Chito-FIONs.[35]

We also investigated whether Chito-FIONs can generate localized tumoricidal effects in response to an external magnetic field. Figure 3c represents the confocal microscopic images of A549 cells following magnetic targeting with Chito-FIONs or Feridex and subsequent applications of an ac magnetic field. The live and dead cells were stained with green fluorescent calcein AM and red fluorescent ethidium homodimer-1, respectively. In the case of A549 cells treated with Chito-FIONs, intense red fluorescence from dead cells was observed inside the area exposed to a magnetic field, whereas no noticeable cell death was detected outside of that area. Since the externally applied magnetic field induced a localized accumulation of Chito-FIONs to the target cells (Figures S7 and S8, Supporting Information), it was conceivable that the

concentrated Chito-FIONs produced localized cytotoxic heat to destroy the cancer cells in a highly selective manner. When the cross-sectional images of the cells were obtained by using a confocal Z-stack method, both Chito-FIONs and Feridex were found to be mostly attached to the cell membrane under applied magnetic field, not localized within the cytoplasm (Figure S9, Supporting Information). Only a marginal level of red fluorescence was observed for the Feridex-treated cells regardless of the applied magnetic field, implying that effective magnetic heating was not achieved by Feridex. It was found that Chito-FIONs exhibited cell viability comparable to Feridex (Figure S10, Supporting Information), indicating that the FIONs themselves did not induce cancer cell death. Moreover, control experiments without applying an ac magnetic field revealed that the observed anticancer activity did not originate from the magnetic targeting of Chito-FIONs to the cells, but was attributed to their magnetically induced hyperthermic effects (Figures S11 and S12, Supporting Information).

We further evaluated the apoptosis-inducing effect of localized hyperthermia treatment with Chito-FIONs and Feridex. To detect the apoptotic activity within cells, a red fluorogenic substrate for caspases 3 and 7 was used. Both caspases 3 and 7 are known as essential proteases, playing central roles in triggering apoptotic processes in mammalian cells.[36] After hyperthermia treatment with Chito-FIONs, only A549 cells in the area exposed to a magnetic field displayed strong red fluorescence throughout the cytoplasm, suggesting that the magnetic targeting of Chito-FIONs significantly enhanced the activation of the caspases in the target cancer cells (Figure 3d). On the other hand, hyperthermia treatment with Feridex did not show any notable change in the cellular apoptotic activity. The extent of cancer cell death was quantitatively measured from the obtained microscopic images (Figure 3e). Chito-FIONs presented a remarkable cytotoxic effect of 78 $\pm$ 9.6% on the cells inside the area exposed to a magnetic field, while a cell death of around 12% was observed outside of that area. There was only a slight enhancement in the cytotoxic effect of Feridex upon application of a magnetic field. When the cellular Fe content was quantified by using inductively coupled plasma absorption emission spectroscopy (ICP-AES), A549 cells treated with Chito-FIONs had a cellular Fe content comparable to those treated with Feridex (Figure S8, Supporting Information). Hence these results revealed that Chito-FIONs induced the thermal destruction of the target cancer cells more efficiently than Feridex with greater activity of facilitating cellular apoptotic processes. To identify whether the cancer cell-killing effect of Chito-FIONs was indeed mediated by an apoptosis mechanism, the apoptotic cell population was also examined (Figure 3f). In the case of A549 cells treated with Chito-FIONs, the apoptotic cell population (95.7 $\pm$ 3.8%) of the cells exposed to a magnetic field was much greater than the value of unexposed cells (27.5 $\pm$ 7.6%), indicating that the apoptotic cell death was mainly responsible for the localized tumoricidal effects of Chito-FIONs.

The therapeutic efficacy of Chito-FIONs was further investigated by monitoring tumor growth in A549 tumor-bearing mice. We administered Chito-FIONs or Feridex (375 μg Fe/kg body weight) intratumorally and then applied an ac magnetic field to the tumor region for 20 min. Since a direct injection allows for the same amount of iron oxide materials to be delivered in a tumor, it was anticipated that the antitumor efficacy of Chito-FIONs and Feridex could be compared at the same level of concentration.[17] It is worthwhile to mention that the amount of iron oxide materials used here (0.21 mg/cm^3 of tumor tissue) was much smaller than those reported in the previous studies (*ca.* 5−10 mg/cm^3 of tumor tissue).[31,37] Notably, the tumor growth was remarkably suppressed by hyperthermia treatment with Chito-FIONs (Figures 4a and S13). While the saline-treated mice showed a tumor volume increase of ~250% in 6 days, a single hyperthermia treatment with Chito-FIONs decreased substantially the tumor volume by about 70%. The tumor growth rates of the Feridex-treated mice were similar to those of the control mice, indicating that hyperthermia treatment with Feridex did not exert any significant tumoricidal effect. The relative tumor volumes for the group treated with Chito-FIONs were greatly regressed by application of an ac magnetic field, whereas notable changes were not observed in the Feridex-treated group (Figure 4b). This suggested that the impressive tumor regression was ascribed to magnetically induced hyperthermic effects of Chito-FIONs. The intratumoral distribution of Chito-FIONs and Feridex was confirmed by histological assessment of the excised tumors (Figures 4c and S14). It was noteworthy that a large amount of Chito-FIONs still remained within the tumor tissue after the hyperthermia treatment, in contrast with only a small residual amount of Feridex within the tumor (Figure S15). Since Chito-FIONs were coated with cationic chitosan oligosaccharides, they would have more positively charged surfaces under acidic tumor microenvironments.[38,39] The enhanced electrostatic interaction between Chito-FIONs and the negatively charged tumor cells might be responsible for the prolonged residence of Chito-FIONs at the tumor tissue. Such high tumor affinity of Chito-FIONs is beneficial for cancer thermotherapy because the target tumors can be irradiated repetitively without further injections of magnetic materials. The anticancer effect of magnetic hyperthermia was also examined by a terminal deoxynucleotidyl transferase-mediated 2′-deoxyuridine 5′-triphosphate-biotin nick end labeling (TUNEL) assay, which detects the tumor region undergoing apoptosis (Figure 4d).

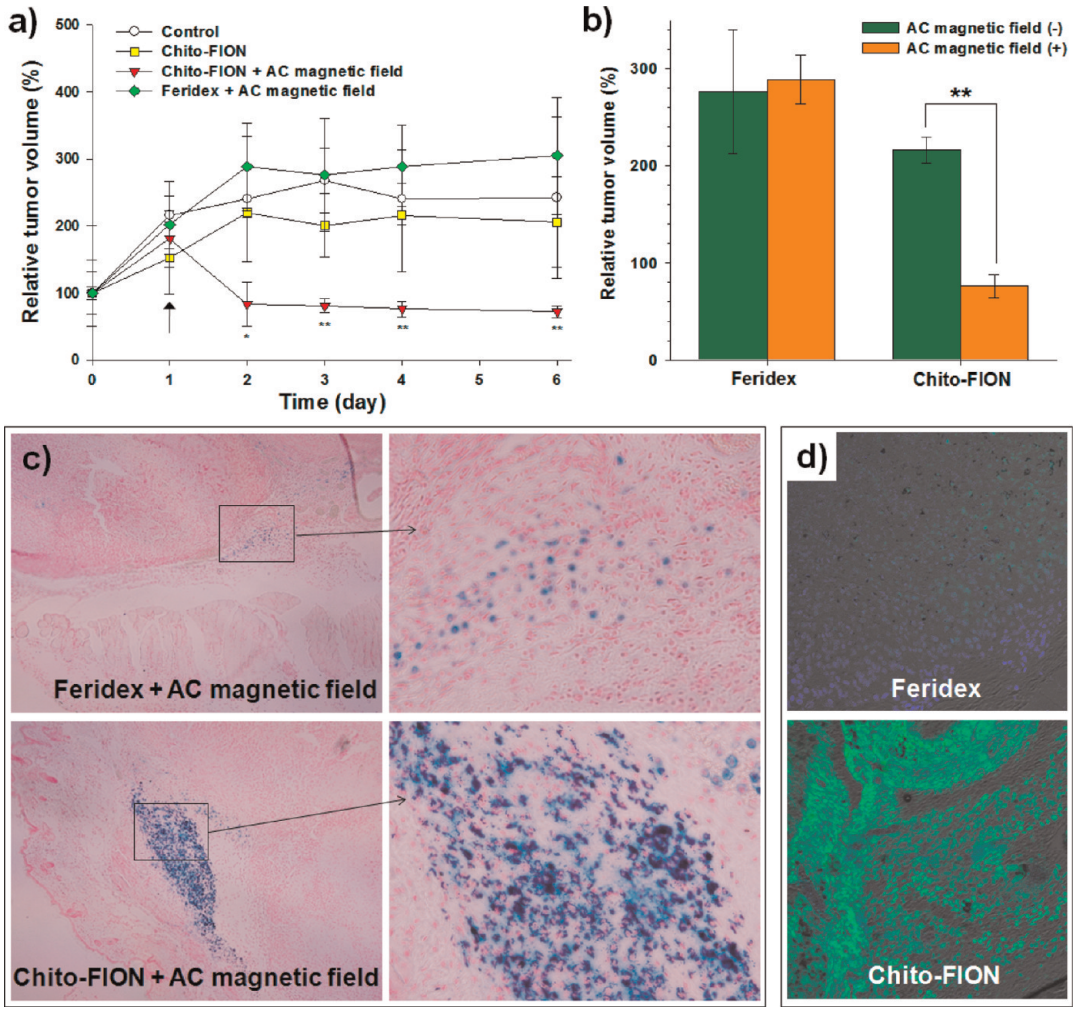

Figure 4. (a) Tumor growth curves of A549 tumor xenografts following a single hyperthermia treatment with Chito-FIONs or Feridex (375 μg Fe/kg body weight). The growth curve of A549 tumors treated with Feridex alone is not shown here for a clear presentation. The arrow represents the day of particle administration. Control groups received saline. Statistically significant difference from controls, *$p < 0.01$, **$p < 0.001$. (b) Relative tumor volume of different treatment groups at day 6. **$p < 0.002$ between two groups. (c) Prussian Blue staining images of tumor sections excised at day 6. The blue region shows the intratumoral distribution of Chito-FIONs and Feridex. (d) Confocal microscopic images of TUNEL-stained tumor sections. Apoptotic cells emit green fluorescence signal. Cell nuclei were also stained with DAPI (blue fluorescence).

Chito-FIONs were shown to promote apoptotic death of cancer cells in the tumor tissues to a far greater extent, as compared to Feridex, showing marginal apoptosis signal. Taken together, the above results demonstrated that Chito-FIONs significantly inhibited tumor growth by triggering apoptotic cell death. Moreover, no significant weight loss was observed in the mice, implying that the hyperthermia treatment with Chito-FIONs was nearly nontoxic despite the pronounced tumoricidal effects (Figure S16, Supporting Information). For clinical applications, a limited range of magnetic field amplitude (H) and frequency (f) should be used to avoid undesirable neuromuscular stimulation and nonspecific inductive heating of normal tissues.[19,37] Generally, ac magnetic fields where the product $H \cdot f$ does not exceed 5×10^9 A m^{-1} s^{-1} are known to be nontoxic to the human body. Since the ac magnetic field used in this study had a relatively small $H \cdot f$ value (6.6×10^8 A m^{-1} s^{-1}), it was conceivable that the hyperthermia treatment with Chito-FIONs could be administered at a safe and tolerable range of magnetic field strengths without causing deleterious side effects.

CONCLUSION

In summary, chitosan-DOPA-stabilized ferrimagnetic iron oxide nanocubes (Chito-FIONs) were developed as an effective heat nanomediator for cancer thermotherapy. A bioinspired surface modification approach using chitosan-DOPA conjugates produced highly stable and water-dispersible ferrimagnetic iron oxide nanocubes. Chito-FIONs exhibited superior magnetic heating ability compared to commercial superparamagnetic iron oxide nanoparticles, leading to successful eradication of cancer cells through caspase-mediated apoptosis. Furthermore, Chito-FIONs

showed excellent antitumor efficacy on an animal tumor model without any severe toxicity. Considering these outstanding characteristics, this novel nanotherapeutic agent combined with magnetic hyperthermia may enable a safe and effective treatment of various types of cancers in the future.

METHODS

Synthesis of 30-nm-Sized Ferrimagnetic Iron Oxide Nanocubes. Synthesis was carried out according to the previously reported procedure.[21] The experiments were conducted in an argon atmosphere using standard Schlenk techniques. In brief, 4 mmol of $Fe(acac)_3$ and 4 mmol of 4-biphenylcarboxylic acid were added to a mixture solution containing 8 mmol of oleic acid and 20.8 g of benzyl ether. The solution was degassed at room temperature for 1 h and then heated to 290 °C at a rate of 20 °C/min with magnetic stirring. The reaction mixture was maintained at this temperature for 30 min. After cooling the solution to room temperature, 50 mL of ethanol and 10 mL of chloroform were added to the solution. The mixture solution was centrifuged at 1700 rpm for 10 min to precipitate the ferrimagnetic iron oxide nanocubes. The separated nanocubes were washed using 50 mL of ethyl alcohol and 10 mL of chloroform.

Synthesis of Chitosan-DOPA-Stabilized Ferrimagnetic Iron Oxide Nanocubes (Chito-FIONs). For synthesis of Chito-FIONs, 0.2 mL of ferrimagnetic iron oxide nanocubes dispersed in chloroform (1.13 mg Fe/mL) was added dropwise to a stirred solution of deionized water (3 mL, pH 7) containing 5 mg of chitosan-DOPA. The solution was sonicated for 3 min by using a Branson sonifier 450 equipped with a microtip (20 kHz, output control 3, duty cycle 40%). The resulting oil-in-water emulsion was subjected to rotary evaporation at 40 °C for 5 min to remove residual solvent under reduced pressure. Excess polymer was removed by dialysis against deionized water for 1 day (M_w cutoff of 12 kDa). For comparison, polyethylene glycol (PEG)-phospholipid-coated FIONs were also prepared according to the previous report.[24]

Measurement of Magnetically Induced Hyperthermic Effect. To evaluate the magnetic heating ability, the samples (Chito-FIONs or Feridex, 150 μg Fe/mL) dispersed in 0.5 mL of 0.1 M PBS solution (pH 7.4) were placed inside a 20-turn copper coil of 1.5 mm thickness and 12.7 mm radius. This coil was connected with resistors (5 Ω) to prepare a resistor−inductor circuit. The magnetic heating was accomplished by using a radio frequency (RF) generator with a linear RF power of 50 W (T&C Power Conversion, Inc., Rochester, NY, USA) that produces an alternating magnetic field with a frequency of 1 MHz and amplitude of 660 A/m. The temperature was monitored automatically with a thermocouple (Woojin Instrument Co., Korea) placed in the center of the sample solution. The specific loss power value of the sample was determined from the initial slope of the temperature *versus* time-dependence curve (dT/dt) normalized to the mass of the magnetic material and the volumetric specific heat capacity of the sample, as described previously.[12]

Magnetic Hyperthermia Treatment and Cytotoxicity Evaluation. Human lung carcinoma A549 cells were seeded on a 35 mm μ-dish (ibidi, Munich, Germany) at a density of 1×10^5 cells per well and incubated for 24 h at 37 °C. The cells were treated with 50 μL of Chito-FIONs or Feridex (150 μg Fe/mL) and then incubated for 12 h at 37 °C either with or without exposing to a cylindrical neodymium magnet (10 mm length, 1.5 mm radius, 3759 G). For hyperthermia treatment, the μ-dish on which the cells were deposited was positioned inside a 20-turn copper coil of 1.5 mm thickness and 18.5 mm radius. The cells were then subjected to an alternating magnetic field for 20 min (frequency, 1 MHz; amplitude, 208 A/m). To assess the proportion of live and dead cells, the treated cells were stained with calcein AM (2 μM) and ethidium homodimer-1 (4 μM) for 30 min. The apoptosis-inducing effect of Chito-FIONs was evaluated by using a Magic Red caspase detection kit, which utilizes a red fluorogenic substrate for caspases 3 and 7. The cell nuclei were also stained with DAPI (1.5 μg/mL in PBS solution) for 10 min. The cells were observed by using a LSM510 confocal laser scanning microscope (Carl Zeiss, Germany).

Conflict of Interest: The authors declare no competing financial interest.

Acknowledgment. All coauthors deeply appreciate invaluable contributions and educational efforts of the late Prof. Tae Gwan Park. T.H. acknowledges the financial support by the Korean Ministry of Education, Science and Technology (MEST) through Strategic Research (2010-0029138), Global Research Laboratory (20110021628), and World Class University (WCU) (R31-10013) Programs of National Research Foundation (NRF) of Korea. T.G.P. acknowledges the financial support by the Korean Ministry for Health, Welfare and Family Affairs, and the WCU program (R31-10071) of MEST. C.G.K. acknowledges the financial support from WCU (R32-20026) of MEST.

Supporting Information Available: Detailed experimental procedure, NMR and FT-IR spectra, TEM images, *etc.*, are described. These material are available free of charge *via* the Internet at http://pubs.acs.org.

REFERENCES AND NOTES

1. Weissleder, R.; Kelly, K.; Sun, E. Y.; Shtatland, T.; Josephson, L. Cell-Specific Targeting of Nanoparticles by Multivalent Attachment of Small Molecules. *Nat. Biotechnol.* **2005**, *23*, 1418–1423.
2. Hao, R.; Xing, R.; Xu, Z.; Hou, Y.; Gao, S.; Sun, S. Synthesis, Functionalization, and Biomedical Applications of Multifunctional Magnetic Nanoparticles. *Adv. Mater.* **2010**, *22*, 2729–2742.
3. Berry, C. C.; Curtis, A. S. G. Functionalisation of Magnetic Nanoparticles for Applications in Biomedicine. *J. Phys. D: Appl. Phys.* **2003**, *36*, R198–R206.
4. Cheon, J.; Lee, J.-H. Synergistically Integrated Nanoparticles as Multimodal Probes for Nanobiotechnology. *Acc. Chem. Res.* **2008**, *41*, 1630–1640.
5. Piao, Y.; Kim, J.; Na, H. B.; Kim, D.; Baek, J. S.; Ko, M. K.; Lee, J. H.; Shokouhimehr, M.; Hyeon, T. Wrap-Bake-Peel Process for Nanostructural Transformation from β-FeOOH Nanorods to Biocompatible Iron Oxide Nanocapsules. *Nat. Mater.* **2008**, *7*, 242–247.
6. Gao, J.; Liang, G.; Cheung, J. S.; Pan, Y.; Kuang, Y.; Zhao, F.; Zhang, B.; Zhang, X.; Wu, E. X.; Xu, B. Multifunctional Yolk-Shell Nanoparticles: A Potential MRI Contrast and Anticancer Agent. *J. Am. Chem. Soc.* **2008**, *130*, 11828–11833.
7. Frey, N. A.; Peng, S.; Cheng, K.; Sun, S. Magnetic Nanoparticles: Synthesis, Functionalization, and Applications in Bioimaging and Magnetic Energy Storage. *Chem. Soc. Rev.* **2009**, *38*, 2532–2542.
8. Ho, D.; Sun, X.; Sun, S. Monodisperse Magnetic Nanoparticles for Theranostic Applications. *Acc. Chem. Res.* **2011**, *44*, 875–882.
9. Park, J.; An, K.; Hwang, Y.; Park, J.-G.; Noh, H.-J.; Kim, J.-Y.; Park, J.-H.; Hwang, N.-M.; Hyeon, T. Ultra-Large-Scale Syntheses of Monodisperse Nanocrystals. *Nat. Mater.* **2004**, *3*, 891–895.
10. Hergt, R.; Dutz, S.; Müller, R.; Zeisberger, M. Magnetic Particle Hyperthermia: Nanoparticle Magnetism and Materials Development for Cancer Therapy. *J. Phys.: Condens. Matter* **2006**, *18*, S2919–S2934.
11. Kumar, C. S.S.R.; Mohammad, F. Magnetic Nanomaterials for Hyperthermia-Based Therapy and Controlled Drug Delivery. *Adv. Drug Delivery Rev.* **2011**, *63*, 789–808.

12. Fortin, J.-P.; Wilhelm, C.; Servais, J.; Ménager, C.; Bacri, J.-C.; Gazeau, F. Size-Sorted Anionic Iron Oxide Nanomagnets as Colloidal Mediators for Magnetic Hyperthermia. *J. Am. Chem. Soc.* **2007**, *129*, 2628–2635.
13. Creixell, M.; Bohorquez, A. C.; Torres-Lugo, M.; Rinaldi, C. EGFR-Targeted Magnetic Nanoparticle Heaters Kill Cancer Cells without a Perceptible Temperature Rise. *ACS Nano* **2011**, *5*, 7124–7129.
14. Derfus, A. M.; von Maltzahn, G.; Harris, T. J.; Duza, T.; Vecchio, K. S.; Ruoslahti, E.; Bhatia, S. N. Remotely Triggered Release from Magnetic Nanoparticles. *Adv. Mater.* **2007**, *19*, 3932–3936.
15. Alphandery, E.; Faure, S.; Seksek, O.; Guyot, F.; Chebbi, I. Chains of Magnetosomes Extracted from AMB-1 Magnetotactic Bacteria for Application in Alternative Magnetic Field Cancer Therapy. *ACS Nano* **2011**, *5*, 6279–6296.
16. Chen, Y.; Bose, A.; Bothun, G. D. Controlled Release from Bilayer-Decorated Magnetoliposomes *via* Electromagnetic Heating. *ACS Nano* **2010**, *4*, 3215–3221.
17. Lee, J.-H.; Jang, J.-T.; Choi, J.-S.; Moon, S. H.; Noh, S.-H.; Kim, J.-W.; Kim, J.-G.; Kim, I.-S.; Park, K. I.; Cheon, J. Exchange-Coupled Magnetic Nanoparticles for Efficient Heat Induction. *Nat. Nanotechnol.* **2011**, *6*, 418–422.
18. Lartigue, L.; Innocenti, C.; Kalaivani, T.; Awwad, A.; Sanchez Duque, M. D. M.; Guari, Y.; Larionova, J.; Guérin, C.; Montero, J.-L. G.; Barragan-Montero, V.; *et al*. Water-Dispersible Sugar-Coated Iron Oxide Nanoparticles. An Evaluation of their Relaxometric and Magnetic Hyperthermia Properties. *J. Am. Chem. Soc.* **2011**, *133*, 10459–10472.
19. Gazeau, F.; Lévy, M.; Wilhelm, C. Optimizing Magnetic Nanoparticle Design for Nanothermotherapy. *Nanomedicine* **2008**, *3*, 831–844.
20. Hirsch, L. R.; Stafford, R. J.; Bankson, J. A.; Sershen, S. R.; Rivera, B.; Price, R. E.; Hazle, J. D.; Halas, N. J.; West, J. L. Nanoshell-Mediated Near-Infrared Thermal Therapy of Tumors under Magnetic Resonance Guidance. *Proc. Natl. Acad. Sci. U. S. A.* **2003**, *100*, 13549–13554.
21. Sanson, C.; Diou, O.; Thevenot, J.; Ibarboure, E.; Soum, A.; Brulet, A.; Miraux, S.; Thiaudiere, E.; Tan, S.; Brisson, A.; *et al*. Doxorubicin Loaded Magnetic Polymersomes: Theranostic Nanocarriers for MR Imaging and Magneto-Chemotherapy. *ACS Nano* **2011**, *5*, 1122–1140.
22. Jang, J.-T.; Nah, H.; Lee, J.-H.; Moon, S. H.; Kim, M. G.; Cheon, J. Critical Enhancements of MRI Contrast and Hyperthermic Effects by Dopant-Controlled Magnetic Nanoparticles. *Angew. Chem., Int. Ed.* **2009**, *48*, 1234–1238.
23. Kim, D.; Lee, N.; Park, M.; Kim, B. H.; An, K.; Hyeon, T. Synthesis of Uniform Ferrimagnetic Magnetite Nanocubes. *J. Am. Chem. Soc.* **2009**, *131*, 454–455.
24. Lee, N.; Kim, H.; Hong, S.; Park, M.; Kim, D.; Kim, H.-C.; Choi, Y.; Lin, S.; Kim, B. H.; Jung, H. S.; *et al*. Magnetosome-Like Ferrimagnetic Iron Oxide Nanocubes for Highly Sensitive MRI of Single Cells and Transplanted Pancreatic Islets. *Proc. Natl. Acad. Sci. U. S. A.* **2011**, *108*, 2662–2667.
25. Amidi, M.; Mastrobattista, E.; Jiskoot, W.; Hennink, W. E. Chitosan-Based Delivery Systems for Protein Therapeutics and Antigens. *Adv. Drug Delivery Rev.* **2010**, *62*, 59–82.
26. Yuk, S. H.; Oh, K. S.; Cho, S. H.; Lee, B. S.; Kim, S. Y.; Kwak, B.-K.; Kim, K.; Kwon, I. C. Glycol Chitosan/Heparin Immobilized Iron Oxide Nanoparticles with a Tumor-Targeting Characteristic for Magnetic Resonance Imaging. *Biomacromolecules* **2011**, *12*, 2335–2343.
27. Lee, H.; Dellatore, S. M.; Miller, W. M.; Messersmith, P. B. Mussel-Inspired Surface Chemistry for Multifunctional Coatings. *Science* **2007**, *318*, 426–430.
28. Xu, C.; Xu, K.; Gu, H.; Zheng, R.; Liu, H.; Zhang, X.; Guo, Z.; Xu, B. Dopamine as a Robust Anchor to Immobilize Functional Molecules on the Iron Oxide Shell of Magnetic Nanoparticles. *J. Am. Chem. Soc.* **2004**, *126*, 9938–9939.
29. Xie, J.; Xu, C.; Kohler, N.; Hou, Y.; Sun, S. Controlled PEGylation of Monodisperse Fe_3O_4 Nanoparticles for Reduced Non-Specific Uptake by Macrophage Cells. *Adv. Mater.* **2007**, *19*, 3163–3166.
30. Ling, D.; Park, W.; Park, Y. I.; Lee, N.; Li, F.; Song, C.; Yang, S.-G.; Choi, S. H.; Na, K.; Hyeon, T. Multiple-Interaction Ligands Inspired by Mussel Adhesive Protein: Synthesis of Highly Stable and Biocompatible Nanoparticles. *Angew. Chem., Int. Ed.* **2011**, *50*, 11360–11365.
31. Pankhurst, Q. A.; Connolly, J.; Jones, S. K.; Dobson, J. Applications of Magnetic Nanoparticles in Biomedicine. *J. Phys. D: Appl. Phys.* **2003**, *36*, R167–R181.
32. Cherukuri, P.; Glazer, E. S.; Curley, S. A. Targeted Hyperthermia using Metal Nanoparticles. *Adv. Drug Delivery Rev.* **2010**, *62*, 339–345.
33. Haase, C.; Nowak, U. Role of Dipole-Dipole Interactions for Hyperthermia Heating of Magnetic Nanoparticle Ensembles. *Phys. Rev. B* **2012**, *85*, 045435.
34. Yoon, T.-J.; Lee, H.; Shao, H.; Hilderbrand, S. A.; Weissleder, R. Multicore Assemblies Potentiate Magnetic Properties of Biomagnetic Nanoparticles. *Adv. Mater.* **2011**, *23*, 4793–4797.
35. Kronast, F.; Friedenberger, N.; Ollefs, K.; Gliga, S.; Tati-Bismaths, L.; Thies, R.; Ney, A.; Weber, R.; Hassel, C.; Römer, F. M.; *et al*. Element-Specific Magnetic Hysteresis of Individual 18 nm Fe Nanocubes. *Nano Lett.* **2011**, *11*, 1710–1715.
36. Earnshaw, W. C.; Martins, L. M.; Kaufmann, S. H. Mammalian Caspases: Structure, Activation, Substrates, and Functions During Apoptosis. *Annu. Rev. Biochem.* **1999**, *68*, 383–424.
37. Moroz, P.; Jones, S. K.; Gray, B. N. Magnetically Mediated Hyperthermia: Current Status and Future Directions. *Int. J. Hyperthermia* **2002**, *18*, 267–284.
38. Fang, N.; Chan, V.; Mao, H. Q.; Leong, K. W. Interactions of Phospholipid Bilayer with Chitosan: Effect of Molecular Weight and pH. *Biomacromolecules* **2001**, *2*, 1161–1168.
39. Yang, R.; Shim, W.-S.; Cui, F.-D.; Cheng, G.; Han, X.; Jin, Q.-R.; Kim, D.-D.; Chung, S.-J.; Shim, C.-K. Enhanced Electrostatic Interaction Between Chitosan-Modified PLGA Nanoparticle and Tumor. *Int. J. Pharm.* **2009**, *371*, 142–147.